Development of Organic and Inorganic Ternary Hybrid Thermoelectric Materials Using Ag Nanoplates

Yukihide Shiraishi*, Satoshi Hoshino*, Keisuke Oshima*, Shinichi Hata*, Yukou Du**, and Naoki Toshima***

Abstract: Thermoelectric technology is used to convert heat energy to electric energy and vice versa, which is an interesting technology to recover electric energy from waste heat. In this study, we focused on a ternary hybrid system consisting of carbon nanotubes, polymers, and Ag nanoplates. The Seebeck coefficient hardly changed even when poly (*N*-vinyl-2-pyrrolidone)(PVP)-protected Ag nanoplates were used. On the other hand, the conductivity was improved by adding the Ag nanoplates. The power factor of the hybrid film in the presence of PVP-Ag nanoplates was 1.2 times higher than that without Ag. Further improvement was achieved by changing the protective agent for the Ag nanoplates from insulating PVP to conductive poly (3,4-ethylenedioxythiophene):poly(styrenesulfonate)(PEDOT:PSS). Based on these results, it was found that the thermoelectric properties were improved by adding the protected Ag nanoplates, especially those protected with PEDOT:PSS.

Key words: Silver Nanoplates, Carbon Nanotubes, Conductive Polymer, Hybrid Thermoelectric Materials

Polymer electronics has currently become an attractive and rapidly growing field.[1] As an alternative to inorganic materials for use in electronics, organic polymer materials have several advantages such as low cost, flexibility, light weight, and printability, and much effort has been devoted to their development for applications including light-emitting diodes,[2,3] transistors,[4,5] touch sensors,[6,7] and photovoltaic cells.[8,9] One of the most widely used polymers in this field is poly (3,4-ethylenedioxythiophene):poly(styrenesulfonate) (PEDOT:PSS) due to its high electrical conductivity. Meanwhile, PEDOT:PSS has recently attracted increasing attention as a p-type organic thermoelectric material.[10-13]

Our group has been studying the development of polymer-based thermoelectric materials.[14-17] The thermoelectric conversion efficiency is defined as the dimensionless figure of merit, i.e. the *ZT* value.

$$ZT = (S^2\sigma/\kappa)T$$

where *S*, σ, κ and *T* are the Seebeck coefficient, electrical conductivity, thermal conductivity and absolute temperature, respectively. Thermoelectric materials with a high *ZT* and power factor, *PF* (=$S^2\sigma$) are desirable, yet there remains a trade-off between the σ and *S*. In the area of thermoelectrics, highly conducting PEDOT:PSS films are also becoming popular and are often used as a p-type thermoelectric material.[18-20] We believe that use of organic-inorganic composite materials is one of the effective routes to improve the thermoelectric properties and consider PEDOT:PSS to be a suitable matrix. For example, we previously reported the thermoelectric properties of the composite thin films of PEDOT:PSS containing

several types of metal nanoparticles as the inorganic component.[14] The effects of the addition of Au nanoparticles with different protecting ligands or different particle shape (spherical or rod) into the PEDOT:PSS film were examined, revealing that some additives can contribute to improvement of the thermoelectric properties, probably due to an increase in the carrier mobility or control of the carrier concentration. Xin *et al.* reported the functionalization of carbon nanotube (CNT) sheet as a flexible substrate by gold nanoplates.[21] On the other hand, Ag nanomaterials have been of interest in the photographic science. In this study, we focused on a ternary hybrid system consisting of PEDOT:PSS, CNTs, and Ag nanoplates.

Silver (I) nitrate ($AgNO_3$), poly (*N*-vinyl-2-pyrrolidone)(PVP, MW ≈ 40000), sodium borohydride, sodium citrate, and hydrogen peroxide were purchased from FUJIFILM Wako Pure Chemical Co., Ltd. The poly (3,4-ethylenedioxythiophene):poly (styrenesulfonate)(PEDOT:PSS) aqueous solution (Clevios™ PH1000; 1 : 2.5 = PEDOT:PSS ratio (w/w)) was purchased from H.C. Starck with the solid content of 1.0-1.3 wt% in water. The polyimide film was kindly supplied by UBE Industries, Ltd., Japan. All chemicals were used without any further purification. Deionized water (18.2 MΩ·cm) was used for all the aqueous solutions. The PVP-protected Ag nanoplates were synthesized by a hydrogen peroxide method.[22] The nominal molar ratio, R=PVP (monomer unit of PVP) / silver (I) nitrate was 0.7. A solution of $AgNO_3$ (0.025 mmol, 4.25 mg) in 0.1 mL PVP aqueous solution (0.0175 mmol in PVP monomer unit), sodium citrate (96.8 mg, 0.375 mmol), 30 wt% hydrogen peroxide (0.06 mL) and H_2O 24.5 mL was stirred under a N_2 atmosphere at

*Department of Applied Chemistry, Sanyo-Onoda City University, Daigakudori, Sanyo-Onoda, Yamaguchi 756-0884, Japan.
**College of Chemistry, Chemical Engineering and Materials Science, Soochow University, Suzhou 215123, PR China.
***Professor Emeritus, Tokyo University of Science Yamaguchi, Japan.
Corresponding author: shiraishi@rs.socu.ac.jp (Y. Shiraishi)

room temperature. An aqueous solution of 0.1M sodium borohydride aq. (0.25 mL, 0.025 mmol) was then rapidly injected into the solution, and the mixture was stirred for 30 min. The PEDOT:PSS-protected Ag nanoplates were prepared in the similar manner. A solution of $AgNO_3$ (0.025 mmol, 4.25 mg) in 0.1 mL PH1000/water (v/v=1/13.6, 0.0175 mmol in PEDOT:PSS monomer unit), sodium citrate (96.8 mg 0.375 mmol), 30 wt% hydrogen peroxide (0.06 mL) and H_2O 24.5 mL was stirred under a N_2 atmosphere at room temperature. An aqueous solution of 0.1M sodium borohydride aq. (0.25 mL, 0.025 mmol) was then rapidly injected into the solution, and the mixture was stirred for 30 min. Total liquid volume was 24.91 mL and then characterized by UV-Vis absorbance measurement. The UV-Vis absorption spectra of the Ag nanoplates were measured by a Shimadzu UV-2500PC recording spectrophotometer using a quartz cell with a 10-mm optical path length. Transmission electron microscopy (TEM) images were obtained by a JEM 1230 instrument (JEOL, Tokyo, Japan) at the accelerated voltage of 80 kV. The TEM sample was prepared by dropping the dispersion solution onto copper grids coated with a thin carbon film.

The PEDOT:PSS / CNT (6/4) hybrid films containing various weight ratios of PVP-protected Ag nanoplates were prepared by the drop-cast method. PEDOT:PSS aqueous solutions (Clevios™ PH1000) containing 0.01-5.0 wt% of Ag nanoplates were sonicated (Ultrasonic Cleaner, TAITEC) for 30 min. Homogeneous Ag nanoplates dispersions with different weight ratios of solids were obtained. One of the Ag nanoplates dispersion (0.8 mL/cm²) was drop-cast on a polyimide sheet, which was placed on a hot plate at 40 ˚C for 12 h. The surface of the film was then covered with a small amount of ethylene glycol (0.24 mL/cm²), dried at 90 ˚C for 12 h, then at 130 ˚C for 30 min,[23,24] resulting in dry PEDOT:PSS / CNT (6/4) hybrid films containing PVP-protected Ag nanoplates with a 5.0±1.0 μm thickness. The thermoelectric properties of the thermoelectric conversion films were measured at least 5 times each by a

ULVAC ZEM-3 M8 instrument (ULVAC-RIKO Inc., Yokohama, Kanagawa, Japan) purged with He at 330-390 K. The PEDOT:PSS / CNT (6/4) hybrid films containing various weight ratios of PEDOT:PSS-protected Ag nanoplates were prepared by the same method.

Colloidal dispersions of the PVP-protected Ag nanoplates were prepared by the Zhang *et al*. reduction method of a mixed solution of silver (I) nitrate and PVP in water.[22] The color of the dispersions of the PVP-protected Ag nanoplates changed from light-yellow to deep-yellow, purple, green, and finally blue after the addition of sodium borohydride. No aggregates or sediments were observed in the prepared PVP-protected Ag nanoplates. The time-dependant UV-vis absorption spectra of the mixture of silver (I) nitrate, PVP, sodium borohydride, sodium citrate, and hydrogen peroxide are shown in Figure 1. Since the solution of silver (I) nitrate has no absorption above 230 nm, the reduction of Ag (I) ions to form PVP-protected Ag nanoparticles can be supported by the absorption at 423 nm due to the plasmon oscillation characteristic of the Ag nanoparticles (Figure 1 yellow line). The intensity of the characteristic peak at 423 nm of the spherical nanoparticles quickly decreased, indicating their decline of nanoparticles during the reaction. At the same time, another peak at 600 nm emerged and gradually red-shifted to longer wavelengths, implying the formation and growth of the Ag nanoplates. The formation and development of Ag nanoplates took about 20-30 min. We previously reported the preparation of PEDOT:PSS-protected noble metal nanoparticles. [25] In this study, we used PEDOT:PSS instead of PVP as a stabilizer of the Ag nanoplates as shown in Figure 2. In Figure 2, yellow line, the absorption spectrum, has the main characteristic peak at 400 nm of the spherical nanoparticles, the shoulder peak at around 330 nm attributed to the out-of-plane quadrupole of Ag nanoplates,[26] and the broadening peak above 500 nm due to PEDOT:PSS itself. The peak at 400 nm is in roughly agreement with PVP-protected Ag nanoparticles. Red-shifts together with broadening of the surface plasmon
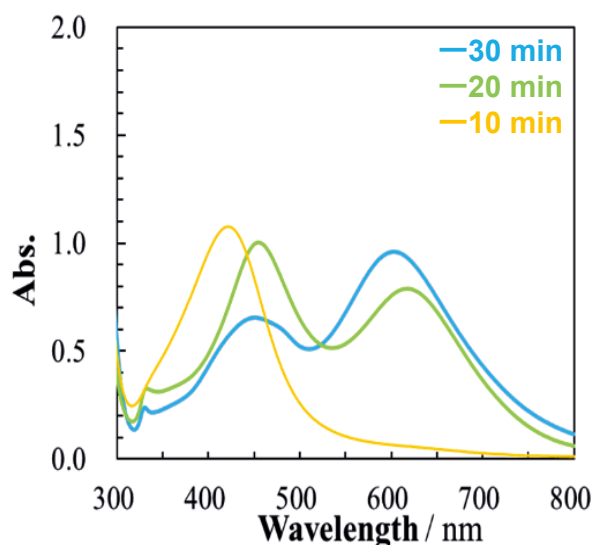

Figure 1 UV-Vis absorption spectra of colloidal dispersions of PVP-protected Ag nanoparticles (yellow line) and Ag nanoplates (green and blue lines).
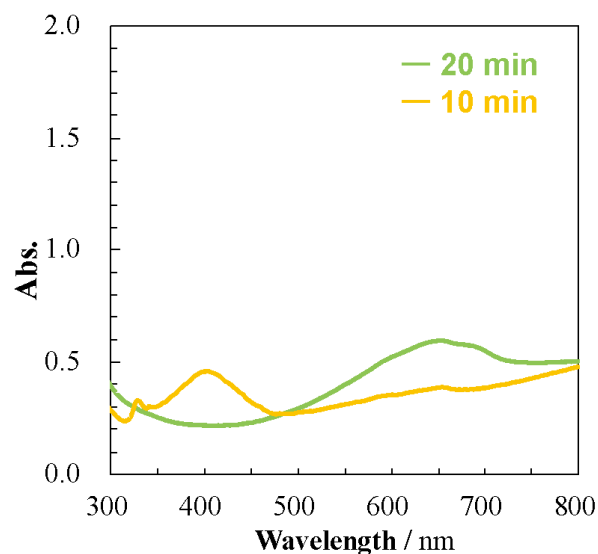

Figure 2 UV-Vis absorption spectra of colloidal dispersions of PEDOT:PSS-protected Ag nanoparticles (yellow line) and Ag nanoplates (green line).

band of Ag particles are observed at 20 min of the reaction time (Figure 2 green line). The disappearance of the shoulder peak at around 330 nm in Figure 2 green line may be due to the diminished thickness of the layer of PEDOT:PSS-protected Ag nanoplates.

Figure 3 shows the transmission electron micrographs and the corresponding histograms indicating the particle size distributions of the PVP-protected Ag nanoplates. Particles in the PVP-protected Ag nanoplates have an average diameter of 19.8 nm and mainly distribute within the range of about 5-25 nm accompanied with small nanoparticles. On the other hand, the average diameter of PEDOT:PSS-protected Ag nanoplates was 28.9 nm and was lager than that of the PVP-protected Ag nanoplates, as shown in Figure 4. The colloidal dispersion of metals can be stabilized by the addition of water-soluble natural or synthetic polymers,[27] surfactants,[28] and organic ligands[29] etc. These stabilizers are called protective colloids or surrounding ligands. In this case, the surrounding ligands can be adsorbed on the surface of metallic nanomaterials, and steric repulsion between the surrounding ligands stabilizes the metallic nanomaterials. The protection ability is expressed by the gold number and the protection value. The protection value of PVP is 50 and is high among the synthetic polymers.[30] On the other hand, the protection ability of PEDOT:PSS for Ag nanoparticles was reported by Dai et al.[31] The protection ability of PVP for metal nanoparticles may be generally stronger than that of PEDOT:PSS. In fact, PVP has been used by many researchers as a protective polymer. The small average diameter of the PVP-protected Ag nanoplates may be due to the highly protective ability.

Recently, Nakai et al. reported that purified semiconducting single-walled CNTs have a high Seebeck coefficient, which made them suitable for use as flexible thermoelectric materials.[32] We investigated the thermoelectric properties of the PEDOT:PSS / CNT hybrid film containing Ag nanoplates using the Seebeck coefficient / electric resistance measurement system. Figure 5 summarizes (a) the Seebeck coefficient S, (b) the electrical conductivity σ, and (c) the power factor PF (=$S^2\sigma$) at 345 K of PEDOT:PSS / CNT films containing various weight ratios of the PVP-protected Ag nanoplates and PEDOT:PSS-protected Ag nanoplates. All of the films show a p-type conduction, and the Seebeck coefficient does not change or only slightly increases with the PVP-protected Ag nanoplates. The electrical conductivity increased from 441 to 519 S cm^{-1} according to the increase in the PVP-protected Ag nanoplates content from 0.0 to 0.01 wt%. The highest power factor, 51.8 μW m^{-1} K^{-2}, was observed at 0.01 wt% PVP-protected Ag nanoplates. Yoshida et al. reported the PEDOT:PSS films containing rod-shaped Au nanorods as organic-inorganic hybrid thermoelectric materials.[14] Salah et al. recently showed that the nanocomposites of ultra-thin copper oxide nanosheets and single-wall carbon nanotubes could be produced and studied for their thermoelectric properties.[33] Incorporating a small amount of CNTs into the matrix of CuO nanosheets enhanced the thermoelectric properties. In general, particles with a large aspect ratio and CNTs can easily build a percolated structure.[34,35] The formation of such a percolated structure gives rise to many connections between the materials and consequently increases the number of paths (network) for carrier transfer, leading to an enhancement of the electrical conductivity.

We next, investigated the thermoelectric properties of the PEDOT:PSS / CNT hybrid film containing PEDOT:PSS-protected Ag nanoplates. The Seebeck coefficient in the presence of the PE-
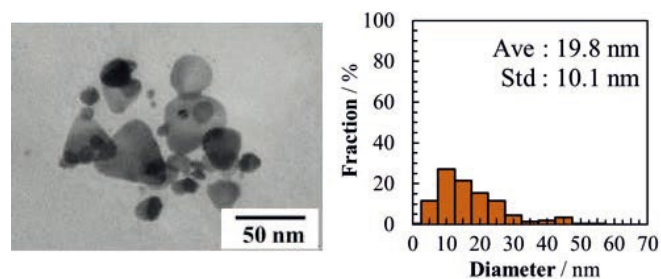

Figure 3 Transmission electron micrograph and particle size histograms of PVP-protected Ag nanoplates. Ave = average diameter, Std = standard deviation.
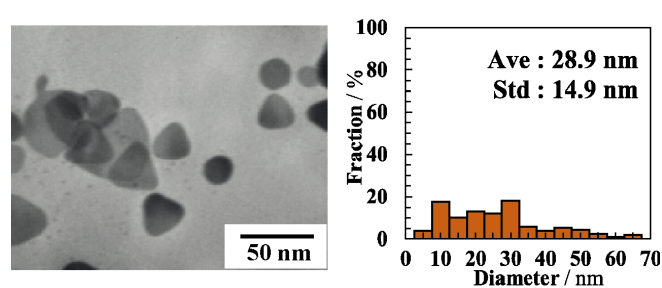

Figure 4 Transmission electron micrograph and particle size histograms of PEDOT:PSS-protected Ag nanoplates. Ave = average diameter, Std = standard deviation.
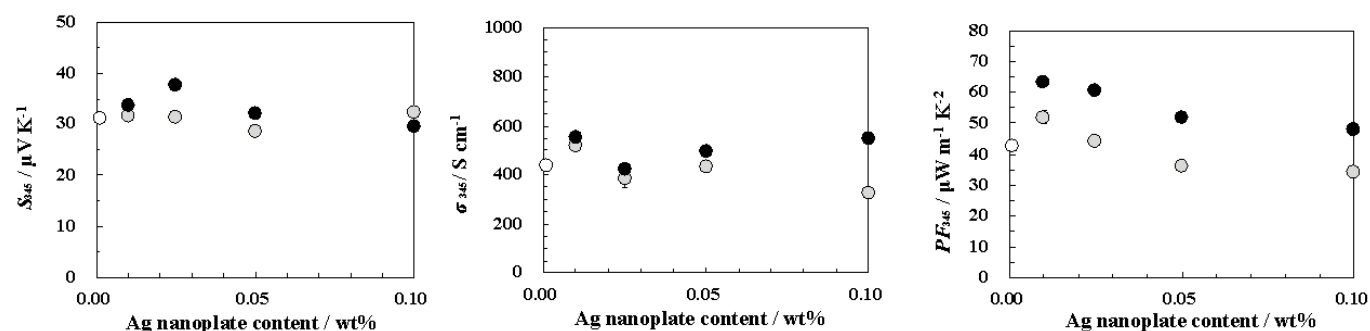

Figure 5 (a) Seebeck coefficient, (b) electrical conductivity and (c) thermoelectric power factor at 345 K of PEDOT:PSS / CNT hybrid film (white) and PEDOT:PSS / CNT hybrid film containing various weight ratios of PVP-protected Ag nanoplates (gray) and PEDOT:PSS-protected Ag nanoplates (black).

DOT:PSS-protected Ag nanoplates (33.7 µV K^{-1}) was almost unchanged. The electrical conductivity of the PEDOT:PSS / CNT films increased from 441 to 554 S cm^{-1} in the presence of the PEDOT:PSS-protected Ag nanoplates. The highest power factor, 63.1 µW m^{-1} K^{-2}, was observed for the 0.01 wt% PEDOT:PSS-protected Ag nanoplates; the carrier flow within the film was accelerated by adding a small amount of the conductive PEDOT:PSS-protected Ag nanoplates. We previously reported the thermoelectric properties of PEDOT:PSS films containing polymer-protected metal nanoparticles.[25] The power factor of PEDOT:PSS films in the presence of PEDOT:PSS-protected Ag nanoparticles(32.0 µW m^{-1} K^{-2}) was larger than that in the absence of Ag nanoparticles (27.8 µW m^{-1} K^{-2}). The improvement rate of power factor in PEDOT:PSS / CNT hybrid films containing PEDOT:PSS-protected Ag nanoplates (1.48 times) was larger than PEDOT:PSS films containing PEDOT:PSS-protected Ag nanoparticles (1.17 times). The electrical conductivity of the films containing the metal nanomaterials with the conductive layer increased with increasing metal concentration, *i.e.*, the power factor improved. Because these results implies that the carrier hopping barrier decreases, i.e. the electrical conductivity increases, in the metal nanoparticles system, PEDOT-PSS-protected metal nanoparticles entered between the PEDOT molecules promoted one-dimensional carrier conduction within PEDOT-PSS films. In this study, we designed a suitable metal-conductive polymer interface within the thermoelectric conversion film and realized a smooth carrier transport by using a small amount of the PEDOT:PSS-protected Ag nanoplates. The films of the ternary organic-inorganic hybrid thermoelectric materials with a high thermoelectric performance can be easily manufactured by drop-casting and drying the corresponding dispersions. Ag nanomaterials have been of interest in the photographic science and will be expected to be applied to new functional materials. Thus, they are expected to be useful for practical applications in the near future.

Acknowledgements

References

1) J. Hanna, J. Soc. Photogr. Sci. Technol. Jpn., **79** (2), 119 (2016).
2) M.C. Gather, A. Köhnen, A. Falcou, H. Becker, K. Meerholz, Adv. Funct. Mater., **17**, 191 (2007).
3) T. Chiba, Y.J. Pu, H. Sasabe, J. Kido, Y. Yang, J. Mater. Chem., **22,** 22769 (2012).
4) T. Someya, T. Sekitani, S. Iba, Y. Kato, H. Kawaguchi, T. Sakurai, Proc. Natl. Acad. Sci. USA, **101**, 9966 (2004).
5) S. Allard, M. Forster, B. Souharce, H. Thiem, U. Scherf, Angew. Chem. Int. Ed., **47**, 4070 (2008).
6) J. Lee, P. Lee, H. Lee, D. Lee, S.S. Lee, S.H. Ko, Nanoscale, **4**, 6408 (2012).
7) S.K. Lim, E.M. Park, J.S. Kim, S.H. Na, H.J. Park, Y.S. Oh, S.J. Suh, Jpn. J. Appl. Phys., **51**, 096501 (2012).
8) S. Günes, H. Neugebauer, N.S. Sariciftci, Chem. Rev., **107**, 1324 (2007).
9) Y. Matsuo, Chem. Lett., **41**, 754 (2012).
10) R.R. Yue, J.K. Xu, Synth. Met., **162**, 912 (2012).
11) O. Bubnova, M. Berggren, X. Crispin, J. Am. Chem. Soc., **134**, 16456 (2012).
12) D. Kim, Y. Kim, K. Choi, J.C. Grunlan, C.H. Yu, ACS Nano, **4**, 513 (2010).
13) F.F. Kong, C.C. Liu, J.K. Xu, Y. Huang, J.M. Wang, Z. Sun, J. Electron. Mater., **41**, 2431 (2012).
14) A. Yoshida, N. Toshima, J. Electron. Mater., **43**, 1492 (2014).
15) N. Toshima, K. Oshima, H. Anno, T. Nishinaka, S. Ichikawa, A. Iwata, Y. Shiraishi, Adv. Mater., **27**, 2246 (2015).
16) Y. Shiraishi, S. Hata, Y. Okawauchi, K. Oshima, H. Anno, N. Toshima, Chem. Lett., **46**, 933 (2017).
17) S. Hata, K. Taguchi, K. Oshima, Y. Du, Y. Shiraishi, N. Toshima, ChemistrySelect, **4**, 6800 (2019).
18) R.R. Yue, J.K. Xu, Synth. Met., **162**, 912 (2012).
19) O. Bubnova, M. Berggren, X. Crispin, J. Am. Chem. Soc., **134**, 16456 (2012).
20) Q. Wei, M. Mukaida, K. Kirihara, Y. Naitoh, T. Ishida, Materials, **8**, 732 (2015).
21) W. Xin, J.-M. Yang, C. Li, M. S. Goorsky, L. Carlson, I. M. D. Rosa, ASC Appl. Mater. Interfaces **9**, 6246 (2017).
22) Q. Zhang, N. Li, J. Goebl, Z. Lu, Y. Yin, J. Am. Chem. Soc., **133**, 18931 (2011).
23) S. Ashizawa, R. Horikawa, H. Okuzaki, Synth. Met., **153**, 5 (2005).
24) D. Hohnholz, H. Okuzaki, A. G. MacDiarmid, Adv. Funct. Mater., **15**, 51 (2005).
25) S. Hata, T. Omura, K. Oshima, Y. Du, Y. Shiraishi, N. Toshima, Bull. Soc. Photogr. Imag. Jpn., **27** (2), 13 (2017).
26) Z. Cao, H. Fu, L. Kang, L. Huang, T. Zhai, Y. Ma, J. Yao, J. Mater. Chem., 18, 2673 (2008).
27) H. Hirai, H. Chawanya, N. Toshima, Reactive Polym., **3**, 127 (1985).
28) C. Petit, A. Taleb, M.P. Pileni, J. Phys. Chem. B, **103**, 1805 (1999).
29) G. Schmid, V. Maihack, F. Lantermann, S. Peschel, J. Chem. Soc. Dalton Transact., 589 (1996).
30) H. Thiele, H. S. von Levern, J. Colloid Sci., **20**, 697 (1965).
31) J. Dai, J. Xu, P. Yang, Y. Du, L. Jiang, Ganguang Kexue Yu Guang Huaxue, **23**, 363 (2005).
32) Y. Nakai, K. Honda, K. Yanagi, H. Kataura, T. Kato, T. Yamamoto, Y. Maniwa, Appl. Phys. Express, **7**, 025103 (2014).
33) N. Salah, N. Baghdadi, A. Alshahrie, A. Saeed, A.R. Ansari, A. Memic, K. Koumoto, J. Euro. Ceramic Soc., **39** (11), 3307 (2019).
34) J. K. W. Sandler, J. E. Kirk, I. A. Kinloch, M. S. P. Shaffer, A. H. Windle, Polymer, **44**, 5893 (2003).
35) G. A. Gelves, B. Lin, U. Sundararaj, J. A. Haber, Adv. Funct. Mater., **16**, 2423 (2006).